

AD-A103 208

AD #103 208

TECHNICAL REPORT ARLCB-TR-81027

TECHNICAL
LIBRARY

STRESS INTENSITY FACTORS FOR RADIAL CRACKS
IN A PARTIALLY AUTOFRETTAGED THICK-WALL CYLINDER

S. L. Pu
M. A. Hussain

July 1981



US ARMY ARMAMENT RESEARCH AND DEVELOPMENT COMMAND
LARGE CALIBER WEAPON SYSTEMS LABORATORY
BENÉT WEAPONS LABORATORY
WATERVLIT, N. Y. 12189

AMCMS No. 611102H600011

DA Project No. 1L161102AH60

PRON No. 1A0215601A1A

APPROVED FOR PUBLIC RELEASE; DISTRIBUTION UNLIMITED

DISCLAIMER

The findings in this report are not to be construed as an official Department of the Army position unless so designated by other authorized documents.

The use of trade name(s) and/or manufacturer(s) does not constitute an official indorsement or approval.

DISPOSITION

Destroy this report when it is no longer needed. Do not return it to the originator.

20. ABSTRACT (CONT'D)

weight functions is found very effective and is used in this report for multiple-radial cracks in a partially autofrettaged tube.

Extensive numerical results are presented for a cylinder having an external diameter twice that of the internal diameter. It is shown that the autofrettaged tube with two diametrically opposed cracks remains, in general, the weakest configuration. For more than two cracks, the higher the number of cracks is, the smaller the stress intensity factor will be.

TABLE OF CONTENTS

	<u>Page</u>
NOMENCLATURE	iii
INTRODUCTION	1
RESIDUAL STRESS AND THERMAL SIMULATION	3
FINITE ELEMENT METHOD	5
METHOD OF LOAD RELIEF FACTOR	10
WEIGHT FUNCTION METHOD	13
NUMERICAL RESULTS	18
CONCLUSIONS	20
REFERENCES	21

TABLES

I. DIMENSIONLESS SIF, $K(p_0)/p_0 \sqrt{\pi c}$, $K(p_1)/p_1 \sqrt{\pi c}$ and $K_c(\epsilon=1)/\sigma_0 \sqrt{\pi c}$ OBTAINED FROM APES FOR A CYLINDER $b = 2$ FOR VARIOUS N AND c/t	9
II. LOAD RELIEF FACTOR $R = K_N/K_{N=2}$ FOR A CYLINDER OF $b = 2$ SUBJECTED TO THREE TYPES OF LOADING	12

LIST OF ILLUSTRATIONS

1(a). A typical finite element idealization.	24
1(b). Idealization for very shallow cracks.	24
2. Stress intensity factors as a function of c/t for N radial cracks subjected to the crack face pressure $p_c(x) = p$.	25
3. Stress intensity factors as a function of c/t for N radial cracks subjected to the crack face pressure $p_c(x) = p(1+x)^{-2}$.	26

	<u>Page</u>
4. Stress intensity factors as a function of c/t for N radial cracks subjected to the crack face pressure $p_c(x) = p \log(1+x)$.	27
5. Stress intensity factors as a function of ϵ in an autofrettaged cylinder of $b = 2$.	28
6. Stress intensity factors as a function of N in a fully autofrettaged cylinder of $b = 2$.	29
7. Stress intensity factors in an autofrettaged cylinder of $b = 2$ subjected to internal pressure σ_0/f on ID and on crack faces.	30

NOMENCLATURE

a	inner radius, used as length unit in this analysis
b	diameter ratio or normalized outer radius
c	normalized depth of cracks
E	Young's modulus of the tube material
K	opening mode stress intensity factors (SIF)
$K(p_0), K(p_i)$	SIF due to uniform tension p_0 and internal pressure p_i
K_c	SIF due to crack face loading p_c
$K_c(p), K_c(pr^{-2})$	SIF due to $p_c = p$, $p_c = pr^{-2}$, respectively
$K_c(\epsilon=0.9)$	SIF due to p_c corresponding to a 90% overstrain residual stress
K_m	SIF for m equally spaced radial cracks emanating from a hole in a infinite plate
$K_{m,f}$	K_m when the infinite plate is replaced by a cylinder of finite thickness
N	number of radial cracks
r, θ	polar coordinates centered at the center of the tube
r_c	radius to the tip of a crack, $r_c = l + c$
t	wall thickness of the cylinder, $t = b - l$
T, T_0, T_ρ	temperature at r , $r = a$ and $r = \rho$, respectively
α	linear thermal expansion coefficient
ϵ	percentage of overstrain, $\epsilon = (\rho - l)/t$, $0 < \epsilon < 1$
ν	Poisson's ratio
ρ	radius of elastic-plastic interface during pressurization
σ_0	uniaxial yield stress of the tube material
σ_r, σ_θ	normal stress in the radial and tangential direction, respectively

INTRODUCTION

In a previous paper,¹ stress intensity factors were obtained, using 12-node quadrilateral, isoparametric elements, for a uniform array of equal depth radial cracks originating at the internal boundary of a pressurized thick-wall cylinder. To increase the maximum pressure a cylinder can contain, it is a common practice to produce a favorable residual stress in the cylinder by an autofrettage process. It is important to find the effect of residual stresses on the stress intensity factor for a cylinder with multiple cracks.

Using the concept of thermal simulation,² the autofrettage residual stresses are simulated by active thermal loads. It is shown that the stress intensity factor for multiple radial cracks in a tube with residual stresses can be computed by the same finite element method.

Slight changes in geometrical configurations or loading conditions require new computations. To obviate this problem, which is a shortcoming of the finite element method, load relief³ and weight function methods^{4,5} are examined. For a small number of radial cracks, the method of load relief enables us to estimate the stress intensity for N other than two fairly accu-

¹Pu, S. L. and Hussain, M. A., "Stress Intensity Factors For a Circular Ring With Uniform Array Radial Cracks Using Isoparametric Singular Elements," ASTM STP-677, 1979, pp. 685-699.

²Hussain, M. A., Pu, S. L., Vasilakis, J. D., and O'Hara, P., "Simulation of Partial Autofrettage by Thermal Loads," Journal of Pressure Vessel Technology, Vol. 102, No. 3, 1980, pp. 314-318.

³Baratta, F. I., "Stress Intensity Factors For Internal Multiple Cracks in Thick-Walled Cylinders Stressed by Internal Pressure Using Load Relief Factors," Engineering Fracture Mechanics, Vol. 10, 1978, pp. 691-697.

⁴Bueckner, H. F., "A Novel Principle For the Computation of Stress Intensity Factors," Z. Agnew. Math. Mech., Vol. 50, 1970, pp. 529-546.

⁵Rice, J. R., "Some Remarks on Elastic Crack-Tip Stress Fields," Int. Journal of Solids and Structures, Vol. 8, 1972, pp. 751-758.

rately by making use of the finite element result for $N = 2$. When N or crack depth is large it is shown in this report that the load relief factor is not reliable because it varies with the nature of the load.

For a given geometrical configuration it is useful to use the weight function method. In the present approach the restrictive assumption that the crack opening displacement is a conic section^{6,7} is circumvented. There are only three types of hoop stress namely: constant, $1/r^2$ and $\log(r)$, in an uncracked cylinder subjected to internal pressure, uniform tension on the outer boundary, and the autofrettage residual stress. This eliminates the need to assume the crack face pressure as a simple polynomial.⁸ It enables us to obtain stress intensity factors for each type of crack face pressure from three linear algebraic equations using three finite element results for the given geometry. The stress intensity factor can be readily calculated for any combination of internal pressure and any degree of autofrettage.

When the radial cracks progress beyond the elastic-plastic interface produced during the autofrettage overstrain, the algebraic equation for stress intensity factor breaks down because the crack face pressure cannot be represented by a simple expression. Modifications are derived for such cases based on the crack opening displacement near a crack tip being parabolic.⁹

⁶Orange, T. W., "Crack Shapes and Stress Intensity Factors for Edge-Cracked Specimens," ASTM STP-513, 1972, pp. 71-78.

⁷Grandt, A. F., "Stress Intensity Factors For Some Through-Cracked Fastener Holes," Int. Journal of Fracture, Vol. 11, 1975, pp. 283-294.

⁸Grandt, A. F., "Stress Intensity Factors For Cracked Holes and Rings Loaded With Polynomial Crack Face Pressure Distributions," Int. Journal of Fracture, Vol. 14, 1978, pp. R221-R229.

⁹Paris, P. C. and Sih, G. C., "Stress Analysis of Cracks," ASTM STP-381, 1965, pp. 39-81.

Extensive numerical results are presented for multiply cracked cylinders having an external diameter twice that of the internal diameter. Results agree with those obtained by other methods for the non-autofrettaged¹⁰ and fully autofrettaged¹¹ cases. In addition, results are given for the partially autofrettaged cases.

RESIDUAL STRESS AND THERMAL SIMULATION

For the case of plane strain, the stress distribution of a partially autofrettaged tube, using the von Mises' yield criterion for the incompressible material, is given by¹²

$$\sigma_r(r) = \begin{cases} \frac{\sigma_0}{\sqrt{3}} \left\{ \left(2 \log \frac{r}{\rho} - 1 + \frac{\rho^2}{b^2} \right) - P_1 \left(\frac{1}{b^2} - \frac{1}{r^2} \right) \right\} & 1 < r < \rho & (1) \\ \frac{\sigma_0}{\sqrt{3}} (\rho^2 - P_1) \left(\frac{1}{b^2} - \frac{1}{r^2} \right) & \rho < r < b & (2) \end{cases}$$

$$\sigma_\theta(r) = \begin{cases} \frac{\sigma_0}{\sqrt{3}} \left\{ 2 \log \frac{r}{\rho} + 1 + \frac{\rho^2}{b^2} - P_1 \left(\frac{1}{b^2} + \frac{1}{r^2} \right) \right\} & 1 < r < \rho & (3) \\ \frac{\sigma_0}{\sqrt{3}} (\rho^2 - P_1) \left(\frac{1}{b^2} + \frac{1}{r^2} \right) & \rho < r < b & (4) \end{cases}$$

¹⁰Tracy, P. G., "Elastic Analysis of Radial Cracks Emanating From the Outer and Inner Surfaces of a Circular Ring," Engineering Fracture Mechanics, Vol. 11, 1979, pp. 291-300.

¹¹Parker, A. P. and Andrasic, C. P., "Stress Intensity Prediction For a Multiply-Cracked, Pressurized Gun Tube With Residual and Thermal Stresses," Presented at Solid Mechanics Symposium, Cape Cod, MA, 1980.

¹²Hill, R., The Mathematical Theory of Plasticity, Oxford at the Clarendon Press, 1950.

where

$$P_1 = P_1(\rho) = \frac{b^2}{b^2-1} \left(1 - \frac{\rho^2}{b^2} + 2 \log \rho\right) \quad (5)$$

If the same hollow cylinder is subjected to a thermal load

$$T(r) = \begin{cases} T_0 - \frac{(T_0-T_\rho)}{\log \rho} \log r & 1 \leq r \leq \rho \\ T_\rho & \rho \leq r \leq b \end{cases} \quad (6)$$

the thermal stresses are given by²

$$\sigma_r(r) = \begin{cases} \frac{E\alpha(T_0-T_\rho)}{2(1-\nu)\log \rho} \left\{ \left(2 \log \frac{r}{\rho} - 1 + \frac{\rho^2}{b^2}\right) - P_1\left(\frac{1}{b^2} - \frac{1}{r^2}\right) \right\} & 1 \leq r \leq \rho \\ \frac{E\alpha(T_0-T_\rho)}{2(1-\nu)\log \rho} (\rho^2-P_1)\left(\frac{1}{b^2} - \frac{1}{r^2}\right) & \rho \leq r \leq b \end{cases} \quad (7)$$

$$\sigma_\theta(r) = \begin{cases} \frac{E\alpha(T_0-T_\rho)}{2(1-\nu)\log \rho} \left\{ 2 \log \frac{r}{\rho} + 1 + \frac{\rho^2}{b^2} - P_1\left(\frac{1}{b^2} + \frac{1}{r^2}\right) \right\} & 1 \leq r \leq \rho \\ \frac{E\alpha(T_0-T_\rho)}{2(1-\nu)\log \rho} (\rho^2-P_1)\left(\frac{1}{b^2} + \frac{1}{r^2}\right) & \rho \leq r \leq b \end{cases} \quad (8)$$

The thermal stresses and the autofrettage residual stresses become equivalent if the temperature gradient of the thermal load and the uniaxial yield stress of the cylinder material have the following relation

$$\frac{E\alpha(T_0-T_\rho)}{2(1-\nu)\log \rho} = \frac{2\sigma_0}{\sqrt{3}} \quad (11)$$

where T_0 or T_ρ may be assigned arbitrarily.

²Hussain, M. A., Pu, S. L., Vasilakis, J. D., and O'Hara, P., "Simulation of Partial Autofrettage by Thermal Loads," Journal of Pressure Vessel Technology, Vol. 102, No. 3, 1980, pp. 314-318.

In many instances there is a redistribution of residual stresses due to changes of geometrical configurations such as the presence of keyways, holes, riflings, and cracks. The stress redistribution may be difficult to find. In case of cracks, it may be difficult to obtain stress intensity factors. For simple problems, the method of superposition may be used to compute the stress redistribution as well as the stress intensity factors involving cracks. Several examples are given in reference 13. An alternative, the thermal simulation method is proposed in reference 2 replacing the residual stress by an active thermal load. The method of thermal simulation shows in reference 13 that the thermal stress redistribution is equivalent to the residual stress redistribution. For more complicated problems, the thermal simulation method has the advantage over the method of superposition by eliminating the computation of residual stresses acting on the surface of the crack which would be present in the uncracked body under external loads. In this report the thermal simulation method is used to compute stress intensity factors for multiple, radial cracks in a fully autofrettaged tube.

FINITE ELEMENT METHOD

The finite element technique has become an important numerical method for practical problems in structural mechanics because of its ability to treat very general geometrical configurations and loading conditions. The trend is

²Hussain, M. A., Pu, S. L., Vasilakis, J. D., and O'Hara, P., "Simulation of Partial Autofrettage by Thermal Loads," Journal of Pressure Vessel Technology, Vol. 102, No. 3, 1980, pp. 314-318.

¹³Pu, S. L. and Hussain, M. A., "Residual Stress Redistribution Caused by Notches and Cracks in a Partially Autofrettaged Tube, Technical Report ARLCB-TR-81005, Benet Weapons Laboratory, LCWSL, ARRADCOM, US Army, January 1981.

to use high order elements requiring a small number of elements for high degree of accuracy. The plane problem of a uniform array of equal depth radial cracks emanating from the bore of a pressurized, non-autofrettaged tube has been solved using 12-node quadrilateral, isoparametric elements.¹ The collapsed singular elements developed by Pu and Hussain¹⁴ are used around the crack tip. The finite element results of stress intensity factors agree well with results in references 15 and 10 using the modified mapping collocation method. Tracy, in a private communication, pointed out a discrepancy of five percent for the case of four cracks with crack depth $c/t = 0.5$ in a tube having outer diameter twice that of inner diameter.

In the previous work,¹ the finite element meshes were automatically generated by a computer program for various values of N and c/t . There is a possibility of excessive distortion of elements for some values of N and c/t . According to Sickles and Gifford,¹⁶ isoparametric elements suffer a loss of accuracy when distorted from a rectangular shape. They recommended a '45 degree rule' as a guide to construct the element mesh. Because of these reasons and our interest in very shallow radial cracks, we have used the

¹Pu, S. L. and Hussain, M. A., "Stress Intensity Factors For a Circular Ring With Uniform Array Radial Cracks Using Isoparametric Singular Elements," ASTM STP-677, 1979, pp. 685-699.

¹⁰Tracy, P. G., "Elastic Analysis of Radial Cracks Emanating From the Outer and Inner Surfaces of a Circular Ring," Engineering Fracture Mechanics, Vol. 11, 1979, pp. 291-300.

¹⁴Pu, S. L. and Hussain, M. A., "The Collapsed Cubic Isoparametric Element as a Singular Element for Crack Problems," International Journal of Numerical Methods in Engineering, Vol. 12, 1978, pp. 1727-1742.

¹⁵Bowie, O. L. and Freese, C. E., "Elastic Analysis For a Radial Crack in a Circular Ring," Journal of Engineering Mechanics, Vol. 4, 1972, pp. 315-321.

¹⁶Sickles, J. B. and Gifford, L. N., "A Further Study of Accuracy Loss in Distorted Isoparametric Finite Elements," DTNSRDC Report M-50, 1979.

enriched quadrilateral elements¹⁷ as crack tip elements in this study. A typical finite element idealization is shown in Figure 1(a). For shallow cracks, the section containing the crack tip changes slightly as shown in Figure 1(b). When thermal simulation is used with the finite element method, the circle $r = \rho$ must be a side of quadrilateral elements in the finite element idealization since thermal loads are different in the two regions of $r < \rho$ and $r > \rho$. The actual finite element idealization for a particular geometry and thermal loads may be modified slightly from those shown in Figure 1.

The finite element computer program APES, an acronym for Axisymmetric/Planar Elastic Structures, is used for all finite element computations in this report. This powerful computer program has been continuously improved with new features including the addition of thermal loading for fracture analysis.¹⁸ The APES results for stress intensity factors for ID radial cracks for a cylinder of $b = 2$ are given in Table I for three types of loading, namely (a) uniform tension p_o on OD, (b) uniform pressure p_i on ID (no crack face pressure) and (c) thermal loading equivalent to a 100 percent overstrain residual stress.² The new results for uniform tension on OD serve as a check to the previously reported results using collapsed singular crack

²Hussain, M. A., Pu. S. L., Vasilakis, J. D., and O'Hara, P., "Simulation of Partial Autofrettage by Thermal Loads," Journal of Pressure Vessel Technology, Vol. 102, No. 3, 1980, pp. 314-318.

¹⁷Gifford, L. N., Jr., "APES - Second Generation Two-Dimensional Fracture Mechanics and Stress Analysis by Finite Elements," DRNSRDC Report 4799. 1975.

¹⁸Gifford, L. N., Jr., "APES - Finite Element Fracture Mechanics Analysis: Revised Documentation," DTNSRDC Report 79/023, 1979.

tip elements.¹ The new results agree within three percent with those reported in references 15 and 10. For instance, the result for $b = 2$, $N = 4$, $c/t = 0.5$, which was $K(p_0)/p_0\sqrt{\pi c} = 2.990$ in reference 1, is now $K(p_0)/p_0\sqrt{\pi c} = 3.149$ which agrees with Tracy's $H_1 = 1.18^{10}$ within 0.1 percent.

An explanation is in order regarding negative stress intensity factors shown in Table I. A crack remains closed in a compressive residual stress region. The stress intensity factor is zero. The crack will open when a sufficiently large internal pressure is applied. The negative value of SIF is convenient in measuring the crack resistance against the opening by internal pressure and it should be understood as such.

The combination of the finite element method and thermal simulation method can be used to compute SIF for any degree of partial autofrettage. However, it is expensive and time consuming to use finite element for parametric studies.

Therefore, we seek alternative methods for the computation of SIF for radial cracks in a partially autofrettaged tube in the following two sections.

¹Pu, S. L. and Hussain, M. A., "Stress Intensity Factors For a Circular Ring With Uniform Array Radial Cracks Using Isoparametric Singular Elements," ASTM STP-677, 1979, pp. 685-699.

¹⁰Tracy, P. G., "Elastic Analysis of Radial Cracks Emanating From the Outer and Inner Surfaces of a Circular Ring," Engineering Fracture Mechanics, Vol. 11, 1979, pp. 291-300.

¹⁵Bowie, O. L. and Freese, C. E., "Elastic Analysis For a Radial Crack in a Circular Ring," Journal of Engineering Mechanics, Vol. 4, 1972, pp. 315-321.

TABLE I. DIMENSIONLESS SIF, $K(p_o)/p_o\sqrt{\pi c}$, $K(p_i)/p_i\sqrt{\pi c}$ and $K_c(\epsilon=1)/\sigma_o\sqrt{\pi c}$
 OBTAINED FROM APES FOR A CYLINDER $b = 2$ FOR VARIOUS N AND c/t

N	Loading	$c/t = 0.05$	$c/t = 0.1$	$c/t = 0.2$	$c/t = 0.3$
1	P_o	2.874	2.825	2.828	2.890
	P_i	1.703	1.711	1.667	1.646
	100% OS	-0.967	-0.896	-0.758	-0.650
2	P_o	2.891	2.874	3.014	3.279
	P_i	1.762	1.745	1.766	1.872
	100% OS	-0.980	-0.919	-0.813	-0.745
3	P_o	2.878	2.860	2.882	3.034
	P_i	1.762	1.731	1.689	1.728
	100% OS	-0.980	-0.907	-0.776	-0.683
4	P_o	2.866	2.826	2.782	2.833
	P_i	1.764	1.710	1.629	1.611
	100% OS	-0.981	-0.895	-0.745	-0.628
6	P_o	2.843	2.753	2.578	2.504
	P_i	1.753	1.665	1.507	1.418
	100% OS	-0.975	-0.871	-0.684	-0.539
10	P_o	2.792	2.590	2.217	2.056
	P_i	1.721	1.566	1.291	1.155
	100% OS	-0.957	-0.817	-0.575	-0.417
20	P_o	2.548	2.062	1.635	1.538
	P_i	1.570	1.243	0.944	0.854
	100% OS	-0.871	-0.641	-0.401	-0.284
30	P_o	2.224	1.687	1.363	1.282
	P_i	1.367	1.014	0.782	0.709
	100% OS	-0.756	-0.515	-0.322	-0.228
40	P_o	1.959	1.465	1.169	1.124
	P_i	1.195	0.879	0.670	0.621
	100% OS	-0.659	-0.442	-0.277	-0.197

METHOD OF LOAD RELIEF FACTOR

Baratta³ extended the coefficient of load relief of Neuber¹⁹ to estimate SIF arising from multiple cracking in a thick-wall cylinder. He defined the ratio

$$R = \frac{K_m}{K_n} \quad (12)$$

as the load relief factors, with K_m and K_n based on a solution due to Tweed and Rooke.²⁰ Assuming that this R value remains nearly constant from an infinitely thick cylinder to a cylinder with finite thickness, he estimated $K_{m,f}$, since $K_{n,f}$ was known for $n = 1$ and $n = 2$ from Bowie and Freese.¹⁵ His estimates, based on the crude assumption, have a discrepancy as high as 20 percent with our finite element results for the same geometry and loading. Parker and Farrow²¹ obtained R values for various numbers of cracks using our results in reference 1. They assumed that R values vary with geometrical configurations, but are independent of loading. Therefore, they obtained SIF for N ID radial cracks for a 100 percent overstrained tube by applying the

¹Pu, S. L. and Hussain, M. A., "Stress Intensity Factors For a Circular Ring With Uniform Array Radial Cracks Using Isoparametric Singular Elements," ASTM STP-677, 1979, pp. 685-699.

³Baratta, F. I., "Stress Intensity Factors For Internal Multiple Cracks in Thick-Walled Cylinders Stressed by Internal Pressure Using Load Relief Factors," Engineering Fracture Mechanics, Vol. 10, 1978, pp. 691-697.

¹⁵Bowie, O. L. and Freese, C. E., "Elastic Analysis For a Radial Crack in a Circular Ring," Journal of Engineering Mechanics, Vol. 4, 1972, pp. 315-321.

¹⁹Neuber, H., "Theory of Notch Stresses," AEC TR 4547, 1958.

²⁰Tweed, J. and Rooke, D. P., "The Stress Intensity Factor For a Crack in Symmetric Array Originating From a Circular Hole in an Infinite Solid," Journal of Engineering Science, Vol. 13, 1975, pp. 653-662.

²¹Parker, A. P. and Farrow, J. R., "Stress Intensity Factors For Multiple Radial Cracks Emanating From the Bore of an Autofrettaged or Thermally Stressed Thick Cylinder," Materials Branch Technical Note MAT/20, Royal Military College of Science, England, 1979.

load relief factors to the solution of SIF for a 100 percent autofrettaged tube with two ID radial cracks due to Grandt.²²

If the load relief factor works for a fully autofrettaged tube, then it should work for a partially overstrained tube also. Our study reveals that R values do vary with the nature of load. Strictly speaking, the concept of load relief factor does not work. However, for a thick wall cylinder subjected to the following three types of loading: (a) uniform tension p_0 on OD, (b) uniform pressure p_i on ID, and (c) residual stress due to 100 percent overstrain, R values vary within \pm five percent except for large values of N and c/t . Table II gives R values for various values of N and c/t under these three types of loading. From Table II it can be seen that R values remain nearly constant for any given N and c/t no matter if the loading is p_0 on OD or p_i on ID. This property enables us to estimate fairly accurately the SIF for p_i from values for p_0 and vice versa. The R values corresponding to the 100 percent overstrain residual stress agree within two percent with R values for p_0 if $N < 4$ and $c/t < 0.3$. Therefore, SIF may be estimated for $N < 4$, $c/t < 0.3$ for partially autofrettaged cases from R values for p_0 and from known results of SIF for $N = 2$ for the same crack depth c/t and loading. The error may exceed ten percent if the load relief factor method is used to estimate SIF for cracked tubes with autofrettage residual stress from R values obtained for p_0 on OD for $N > 10$ and $c/t > 0.2$. For loading conditions other than the three types mentioned, the method of load relief factor should be applied with care.

²²Grandt, A. F., "Two Dimensional Stress Intensity Factor Solutions For Radially Cracked Rings," Technical Report AFML-TR-75-121, Air Force Materials Laboratory, Wright-Patterson Air Force Base, 1975.

TABLE II. LOAD RELIEF FACTOR $R = K_N/K_{N=2}$ FOR A CYLINDER OF $b = 2$

SUBJECTED TO THREE TYPES OF LOADING

N	Loading	c/t = 0.05	c/t = 0.1	c/t = 0.2	c/t = 0.3
1	P _o	0.994	0.983	0.938	0.881
	P _i	0.967	0.980	0.943	0.897
	100% OS	0.987	0.976	0.932	0.873
3	P _o	0.996	0.995	0.956	0.925
	P _i	1.000	0.992	0.956	0.923
	100% OS	1.000	0.987	0.954	0.918
4	P _o	0.992	0.983	0.923	0.864
	P _i	1.002	0.980	0.922	0.860
	100% OS	1.002	0.974	0.917	0.844
6	P _o	0.984	0.958	0.855	0.764
	P _i	0.995	0.954	0.853	0.757
	100% OS	0.995	0.948	0.841	0.723
10	P _o	0.966	0.901	0.735	0.627
	P _i	0.977	0.897	0.731	0.617
	100% OS	0.977	0.889	0.707	0.560
20	P _o	0.882	0.718	0.543	0.469
	P _i	0.891	0.713	0.534	0.456
	100% OS	0.889	0.697	0.493	0.381
30	P _o	0.769	0.587	0.452	0.391
	P _i	0.776	0.581	0.443	0.379
	100% OS	0.772	0.561	0.396	0.307
40	P _o	0.678	0.510	0.388	0.343
	P _i	0.678	0.504	0.379	0.331
	100% OS	0.672	0.481	0.340	0.264

WEIGHT FUNCTION METHOD

Bueckner⁴ and Rice⁵ have shown that knowledge of the SIF and displacement field for a flaw geometry enables construction of a weight function which depends only on geometry. With the weight function method, one may obtain SIF for any other symmetric loading applied to the same geometry. Grandt has applied this technique to obtain SIF for a large plate containing radial hole cracks⁷ and for radially cracked rings²² loaded with arbitrary symmetric crack pressure. The SIF K for a specified crack face loading $p_c(x)$, based on the weight function approach, is given by

$$K = \frac{H}{K^*} \int_0^c p_c(x) \frac{\partial v}{\partial c} dx \quad (13)$$

where H is a constant, $H = E$ for plane stress and $H = E/(1-\nu^2)$ for plane strain, K^* is the known SIF for a given loading applied to the flaw geometry of interest, x is the distance from the edge of the hole, v is the crack opening profile corresponding to the known SIF K^* . In Eq. (13) the only undefined term is the partial derivative $\partial v/\partial c$. The finite element results of the y -component of displacement at nodal points along the crack face are not enough for the determination of the crack profile. Grandt used the assumption

⁴Bueckner, H. F., "A Novel Principle For the Computation of Stress Intensity Factors," *Z. Agnew. Math. Mech.*, Vol. 50, 1970, pp. 529-546.

⁵Rice, J. R., "Some Remarks on Elastic Crack-Tip Stress Fields," *Int. Journal of Solids and Structures*, Vol. 8, 1972, pp. 751-758.

⁷Grandt, A. F., "Stress Intensity Factors For Some Through-Cracked Fastener Holes," *Int. Journal of Fracture*, Vol. 11, 1975, pp. 283-294.

²²Grandt, A. F., "Two Dimensional Stress Intensity Factor Solutions For Radially Cracked Rings," Technical Report AFML-TR-75-121, Air Force Materials Laboratory, Wright-Patterson Air Force Base, 1975.

of conic sections due to Orange.⁶ Andrasic and Parker²³ used the method of virtual crack extension²⁴ and B-spline curve fitting. In this report the loading of the cracked tube is limited to a combination of internal pressure and the autofrettage residual stresses. A set of algebraic equations is used in lieu of the determination of $\partial v/\partial c$.

The crack face loading $p_c(x)$ in Eq. (13) for a cracked tube subjected to the autofrettage residual stress is given by the hoop stress, Eqs. (3) and (4), for an uncracked, overstrained tube

$$\frac{p_c(x)}{\sigma_o} = \frac{\sigma_\theta(x)}{\sigma_o} = \begin{cases} \frac{1}{\sqrt{3}} [(2-P_1) - P_1(1+x)^{-2} + 2 \log(1+x)] & 0 \leq x \leq \epsilon t \quad (14) \\ \frac{1}{\sqrt{3}} [(\rho^2-P_1)b^{-2} + (\rho^2-P_1)(1+x)^{-2}] & \epsilon t \leq x \leq t \quad (15) \end{cases}$$

For $\epsilon = 1$, substituting from Eq. (14) into Eq. (13), the following is obtained:

$$\frac{K_c(\epsilon=1)}{\sigma_o\sqrt{\pi c}} = \frac{1}{\sqrt{3\pi c}} [\{2 - P_1(b)\} K_c(1) - P_1(b) K_c(r^{-2}) + 2K_c(\log r)] \quad (16)$$

where

$$K_c(1) = \frac{H}{K^*} \int_0^c \frac{\partial v}{\partial c} dx \quad (17)$$

⁶Orange, T. W., "Crack Shapes and Stress Intensity Factors for Edge-Cracked Specimens," ASTM STP-513, 1972, pp. 71-78.

²³Andrasic, C. P. and Parker, A. P., "Weight Functions For Cracked Curved Beams," Second International Conference on Numerical Methods in Fracture Mechanics, Swansea, U.K., 1980.

²⁴Parks, D. M. and Kamenetzky, E. M., "Weight Functions From Virtual Crack Extensions," International Journal For Numerical Methods in Engineering, Vol. 14, 1979, pp. 1693-1706.

$$K_C(r^{-2}) = \frac{H}{K^*} \int_0^c (1+x)^{-2} \frac{\partial v}{\partial c} dx \quad (18)$$

$$K_C(\log r) = \frac{H}{K^*} \int_0^c [\log(1+x)] \frac{\partial v}{\partial c} dx \quad (19)$$

These may be termed as functional intensity factors.

From the Lamé' solution, the hoop stress in an uncracked cylinder subjected to uniform tension p_0 on OD is

$$\frac{\sigma_\theta}{p_0} = \frac{b^2}{b^2-1} \left(1 + \frac{1}{r^2}\right) \quad (20)$$

The same stress under internal pressure p_i is

$$\frac{\sigma_\theta}{p_i} = \frac{1}{b^2-1} \left(1 + \frac{b^2}{r^2}\right) \quad (21)$$

Substituting σ_θ for p_C in Eq. (13), the SIF for a radially cracked cylinder subjected to p_0 or p_i is given by one of the following

$$\frac{K(p_0)}{p_0\sqrt{\pi c}} = \frac{b^2}{b^2-1} \frac{K_C(1)}{\sqrt{\pi c}} + \frac{b^2}{b^2-1} \frac{K_C(r^{-2})}{\sqrt{\pi c}} \quad (22)$$

$$\frac{K(p_i)}{p_i\sqrt{\pi c}} = \frac{1}{b^2-1} \frac{K_C(1)}{\sqrt{\pi c}} + \frac{b^2}{b^2-1} \frac{K_C(r^{-2})}{\sqrt{\pi c}} \quad (23)$$

If the left hand sides of Eqs. (22) and (23) are numerically determined from the finite element method, then $K_C(1)$ and $K_C(r^{-2})$ can be solved. Inserting these values into Eq. (16), $K_C(\log r)$ can be solved if $K_C(\epsilon=1)$ is known from the finite element computation.

Once $K_C(1)$, $K_C(r^{-2})$, and $K_C(\log r)$ are known for a given geometry (b , N , c/t are fixed), the SIF for the flawed cylinder subjected to a residual stress

corresponding to a given ϵ ($\neq 1$) can be computed from

$$\frac{K_c(\epsilon)}{\sigma_0 \sqrt{\pi c}} = \frac{1}{\sqrt{3\pi c}} [\{2 - P_1(\rho)\} K_c(1) - P_1(\rho) K_c(r^{-2}) + 2K_c(\log r)] \quad (24)$$

provided $c \leq \epsilon t$.

In case $c > \epsilon t$, the crack face pressure is a combination of Eqs. (14) and (15); therefore, Eq. (24) is not valid. If $c/t = \epsilon + \delta$ and $0 < \delta \ll 1$, we may use Eq. (24) to compute an approximate SIF and then use the following equation to compute a corrective SIF, K_δ

$$\frac{K_\delta}{\sigma_0 \sqrt{\pi c}} = \frac{1}{\sqrt{3\pi c}} \frac{H}{K^*} \int_{\epsilon t}^{(\epsilon + \delta)t} p_c(x) \frac{\partial v}{\partial c} dx \quad (25)$$

where

$$p_c(x) = (-1 + 2 \log \rho) + \rho^2(1+x)^{-2} - 2 \log(1+x) \quad (26)$$

The final result of SIF for a small $\delta > 0$ is the sum of $K_c(\epsilon)$, Eq. (24), and K_δ , Eq. (25).

An approximate method for K_δ is based on the Westergaard near field solution.²⁵ The crack opening displacement $v(\xi)$ near a crack tip due to an arbitrary load is given in terms of SIF K^* at the crack tip by

$$v(\xi) = \frac{2K^*}{H} \left(\frac{2\xi}{\pi} \right)^{1/2} \quad (27)$$

The derivative with respect to the crack length is

$$\frac{\partial v}{\partial c} = \frac{K^*}{H} \left(\frac{2}{\pi} \right)^{1/2} (\xi^{-1/2} + \xi^{1/2}/c) \quad (28)$$

²⁵Westergaard, H. M., "Bearing Pressures and Cracks," Transactions of the ASME, Journal of Applied Mechanics, 1939.

The length variable ξ is defined by

$$\xi = -(x-c) \quad (29)$$

Substituting from Eqs. (26) and (28) into (25) and using Eq. (29), we have

$$\frac{K_\delta}{\sigma_0 \sqrt{\pi c}} = \frac{1}{\sqrt{3\pi c}} \sqrt{2/\pi} \{(-1 + 2 \log \rho)(I_1 + I_1') + \rho^2(I_2 + I_2') - 2(I_3 + I_3')\} \quad (30)$$

where

$$I_1 = 2\sqrt{\delta t} \quad , \quad I_1' = \frac{2}{3c} (\delta t)^{3/2} \quad (31)$$

$$I_2 = \frac{1}{1+c} \left[\frac{\sqrt{\delta t}}{\rho} - \frac{(1+c)^{-1/2}}{2} \log D(\rho) \right] \quad (32)$$

$$I_2' = \frac{1}{c} \left[\frac{\sqrt{\delta t}}{\rho} + \frac{(1+c)^{-1/2}}{2} \log D(\rho) \right]$$

$$I_3 = -2[(2-\log \rho)\sqrt{\delta t} + (1+c)^{1/2} \log \frac{\sqrt{1+c} - \sqrt{\delta t}}{\sqrt{1+c} + \sqrt{\delta t}}] \quad (33)$$

$$I_3' = \frac{2}{3c} [\sqrt{\delta t}(\delta t\{\log \rho - 2(1+c) - 2\delta t/3\}) - (1+c)^{3/2} \log D(\rho)]$$

with

$$D(\rho) = [2(1+c) - \rho - 2\sqrt{\delta t(1+c)}]/\rho \quad (34)$$

It should be noted that Eq. (30) is independent of N . It works for small N and δ . If N is small, it may work for a relatively larger δ . But when N is large, the crack interaction is strong, δ must be small.

NUMERICAL RESULTS

Using Eqs. (16), (22), and (23) and finite element results in Table I, we obtain values of $K_C(p)/p\sqrt{\pi c}$, $K_C(pr^{-2})/p\sqrt{\pi c}$, and $K_C(p \log r)/p\sqrt{\pi c}$. Figures 2 through 4 are plots of these values as a function of c/t for various values of N . The use of these graphs and Eq. (24) gives $K_C(\epsilon)/\sigma_0\sqrt{\pi c}$ for any value of ϵ , $\epsilon t > c$, for a given geometry. A graph of $K_C(\epsilon)/\sigma_0\sqrt{\pi c}$ versus ϵ is shown in Figure 5 for various c/t and for $N = 2$ and $N = 40$. Figure 6 is another way of presenting $K_C(\epsilon)/\sigma_0\sqrt{\pi c}$ in which ϵ is fixed but N varies.

The numerical results given previously are enough for an estimate of SIF for any assigned values of N , c/t , and ϵ . For example, if the SIF is desired for $N = 8$, $c/t = 0.15$, and $\epsilon = 0.75$, readings are taken from Figures 2 through 4 as follows: $K_C(p)/p\sqrt{\pi c} = 1.03$, $K_C(pr^{-2})/p\sqrt{\pi c} = 0.86$, and $K_C(p \log r)/p\sqrt{\pi c} = 0.091$. For $\epsilon = 0.75$ we have from Eqs. (5) and (24) $K_C(\epsilon = 0.75)/\sigma_0\sqrt{\pi c} = -0.67$. In another example, if the SIF for $N = 2$, $c/t = 0.30$ and $\epsilon = 0.25$ is desired, we first compute $K_C(\epsilon = 0.25)/\sigma_0\sqrt{\pi c}$ from Eq. (24) with $K_C(1)/\sqrt{\pi c} = 1.41$ from Figure 2, $K_C(r^{-2})/\sqrt{\pi c} = 1.05$ from Figure 3, and $K_C(\log r)/\sqrt{\pi c} = 0.22$ from Figure 4. The result from Eq. (24) is $K_C(\epsilon = 0.25)/\sigma_0\sqrt{\pi c} = -0.12$. In this case since $c/t > \epsilon$, we have to compute $K_\delta/\sigma_0\sqrt{\pi c}$ from Eqs. (30) through (34) with $\delta t = 0.05$. The corrective SIF is $K_\delta/\sigma_0\sqrt{\pi c} = -0.023$ and the desired SIF is $K_C(\epsilon = 0.25)/\sigma_0\sqrt{\pi c} = -0.143$. A finite element computation is performed for the case; the result is also -0.143 . If in the previous example $\epsilon = 0.20$ is desired, i.e., $\delta t = 0.1$, Eq. (24) gives $K_C/\sigma_0\sqrt{\pi c} = -0.0209$ and Eq. (30) gives $K_\delta/\sigma_0\sqrt{\pi c} = -0.0668$. The final result is $K_C(\epsilon = 0.2)/\sigma_0\sqrt{\pi c} = -0.088$ which is 5.6 percent less than the finite element result $K_C(\epsilon = 0.2)/\sigma_0\sqrt{\pi c} = -0.093$. This indicates that δ must be fairly small for Eq. (30) to be valid.

For the geometry $N = 10$, $c/t = 0.3$, the finite element computation gives $K_C(\epsilon = 0.3)/\sigma_0\sqrt{\pi c} = -0.079$ and $K_C(\epsilon = 0.25)/\sigma_0\sqrt{\pi c} = -0.044$. The corresponding values computed from Eq. (24) and from Eqs. (24) and (30) are -0.080 and -0.0477 .

The stress intensity factors due to a combination of residual stress and internal pressure on ID and on crack faces can be readily computed by linear superposition. If the applied pressure is $p_i = \sigma_0/f$, where f is a constant, the resultant SIF's for $f = 1.5$ and 3 , for $N = 1$ and 40 , and for $\epsilon = 1.0$ are shown in Figure 7. We purposely keep the negative SIF for shallow cracks in the case of $f = 3$ and $\epsilon = 1.0$. The correct SIF should be zero, which means that a single crack or a set of multiple cracks remains closed due to the high compressive residual stress near the bore. The negative SIF gives a little more information than $SIF = 0$. The graph also shows a higher SIF for $N = 1$ than that for $N = 40$ for a given ϵ and f . One may conclude that it is worse to have a single radial crack than to have a large number of radial cracks in an autofrettaged tube. This conclusion is similar to that found in the study of non-autofrettaged tubes. With some slight modification, the method used here can be applied to multiple OD cracks. The modifications and numerical results for OD cracks are to be reported elsewhere.

CONCLUSIONS

The finite element method together with the thermal simulation method can be used to compute the stress intensity factor for multiple radial cracks emanating from the bore of a partially autofrettaged tube. The finite element results of $K(p_0)$, $K(p_1)$, and $K_c(\epsilon = 1.0)$ can lead to a system of algebraic equations for solving $K_c(1)$, $K_c(r^{-2})$, and $K_c(\log r)$. Using these results the weight function concept gives an alternative method for the determination of SIF for any degree of partial autofrettage provided that the crack depth c/t is not greater than the percentage of autofrettage ϵ . A correction formula is supplied for the SIF when c/t is slightly greater than ϵ when N is small. These expressions yield quite accurate results and can save a great deal of computing time.

The useful tube life is prolonged because of the autofrettage process. The cylinder with two diametrically opposed cracks remains in general the weakest configuration. For more than two cracks, the stress intensity factor decreases as the number of cracks increases. The fatigue life is longer for cylinders with more radial cracks.

REFERENCES

1. Pu, S. L. and Hussain, M. A., "Stress Intensity Factors For a Circular Ring With Uniform Array of Radial Cracks Using Isoparametric Singular Elements," ASTM STP-677, 1979, pp. 685-699.
2. Hussain, M. A., Pu, S. L., Vasilakis, J. D., and O'Hara, P., "Simulation of Partial Autofrettage by Thermal Loads," Journal of Pressure Vessel Technology, Vol. 102, No. 3, 1980, pp. 314-318.
3. Baratta, F. I., "Stress Intensity Factors For Internal Multiple Cracks in Thick-Walled Cylinders Stressed by Internal Pressure Using Load Relief Factors," Engineering Fracture Mechanics, Vol. 10, 1978, pp. 691-697.
4. Bueckner, H. F., "A Novel Principle For the Computation of Stress Intensity Factors," Z. Angew. Math. Mech., Vol. 50, 1970, pp. 529-546.
5. Rice, J. R., "Some Remarks on Elastic Crack-Tip Stress Fields," Int. Journal of Solids and Structures, Vol. 8, 1972, pp. 751-758.
6. Orange, T. W., "Crack Shapes and Stress Intensity Factors for Edge-Cracked Specimens," ASTM STP-513, 1972, pp. 71-78.
7. Grandt, A. F., "Stress Intensity Factors For Some Through-Cracked Fastener Holes," Int. Journal of Fracture, Vol. 11, 1975, pp. 283-294.
8. Grandt, A. F., "Stress Intensity Factors For Cracked Holes and Rings Loaded With Polynomial Crack Face Pressure Distributions," Int. Journal of Fracture, Vol. 14, 1978, pp. R221-R229.
9. Paris, P. C. and Sih, G. C., "Stress Analysis of Cracks," ASTM STP-381, 1965, pp. 39-81.

10. Tracy, P. G., "Elastic Analysis of Radial Cracks Emanating From the Outer and Inner Surfaces of a Circular Ring," *Engineering Fracture Mechanics*, Vol. 11, 1979, pp. 291-300.
11. Parker, A. P. and Andrasic, C. P., "Stress Intensity Prediction For a Multiply-Cracked, Pressurized Gun Tube With Residual and Thermal Stresses," Presented at Solid Mechanics Symposium, Cape Cod, MA, 1980.
12. Hill, R., The Mathematical Theory of Plasticity, Oxford at the Clarendon Press, 1950.
13. Pu, S. L. and Hussain, M. A., "Residual Stress Redistribution Caused by Notches and Cracks in a Partially Autofrettaged Tube," Technical Report ARLCB-TR-81005, Benet Weapons Laboratory, LCWSL, ARRADCOM, US Army, January 1981.
14. Pu, S. L. and Hussain, M. A., "The Collapsed Cubic Isoparametric Element as a Singular Element for Crack Problems," *International Journal of Numerical Methods in Engineering*, Vol. 12, 1978, pp. 1727-1742.
15. Bowie, O. L. and Freese, C. E., "Elastic Analysis For a Radial Crack in a Circular Ring," *Journal of Engineering Mechanics*, Vol. 4, 1972, pp. 315-321.
16. Sickles, J. B. and Gifford, L. N., "A Further Study of Accuracy Loss in Distorted Isoparametric Finite Elements," DTNSRDC Report M-50, 1979.
17. Gifford, L. N., Jr., "APES - Second Generation Two-Dimensional Fracture Mechanics and Stress Analysis by Finite Elements," DTNSRDC Report 4799, 1975.

18. Gifford, L. N. Jr., "APES - Finite Element Fracture Mechanics Analysis: Revised Documentation," DTNSRDC Report 79/023, 1979.
19. Neuber, H., "Theory of Notch Stresses," AEC TR 4547, 1958.
20. Tweed, J. and Rooke, D. P., "The Stress Intensity Factor For a Crack in Symmetric Array Originating From a Circular Hole in an Infinite Solid," Journal of Engineering Science, Vol. 13, 1975, pp. 653-662.
21. Parker, A. P. and Farrow, J. R., "Stress Intensity Factors For Multiple Radial Cracks Emanating From the Bore of an Autofrettaged or Thermally Stressed Thick Cylinder," Materials Branch Technical Note MAT/20, Royal Military College of Science, England, 1979.
22. Grandt, A. F., "Two Dimensional Stress Intensity Factor Solutions For Radially Cracked Rings," Technical Report AFML-TR-75-121, Air Force Materials Laboratory, Wright-Patterson Air Force Base, 1975.
23. Andrasic, C. P. and Parker, A. P., "Weight Functions for Cracked Curved Beams," Second International Conference on Numerical Methods in Fracture Mechanics, Swansea, U.K., 1980.
24. Parks, D. M. and Kamenetzky, E. M., "Weight Functions From Virtual Crack Extensions," International Journal For Numerical Methods in Engineering, Vol. 14, 1979, pp. 1693-1706.
25. Westergaard, H. M., "Bearing Pressures and Cracks," Transactions of the ASME, Journal of Applied Mechanics, 1939.

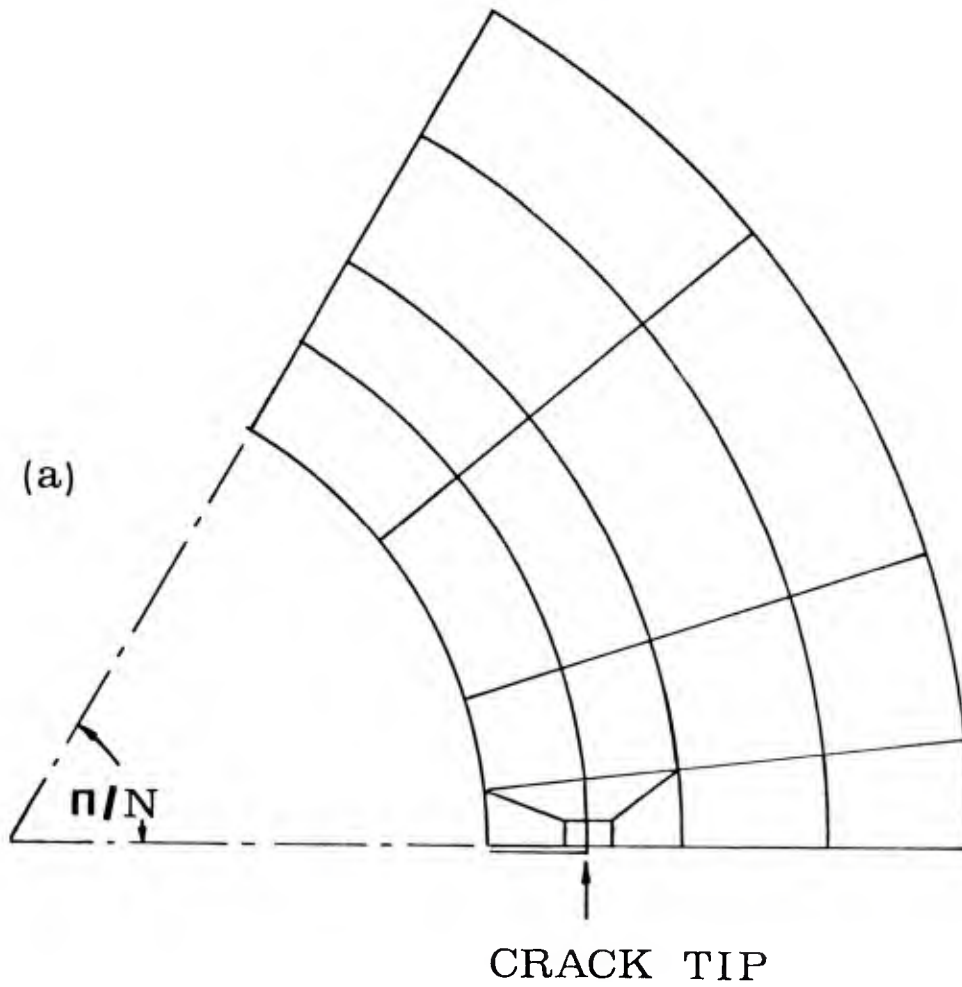


Figure 1(a). A typical finite element idealization.

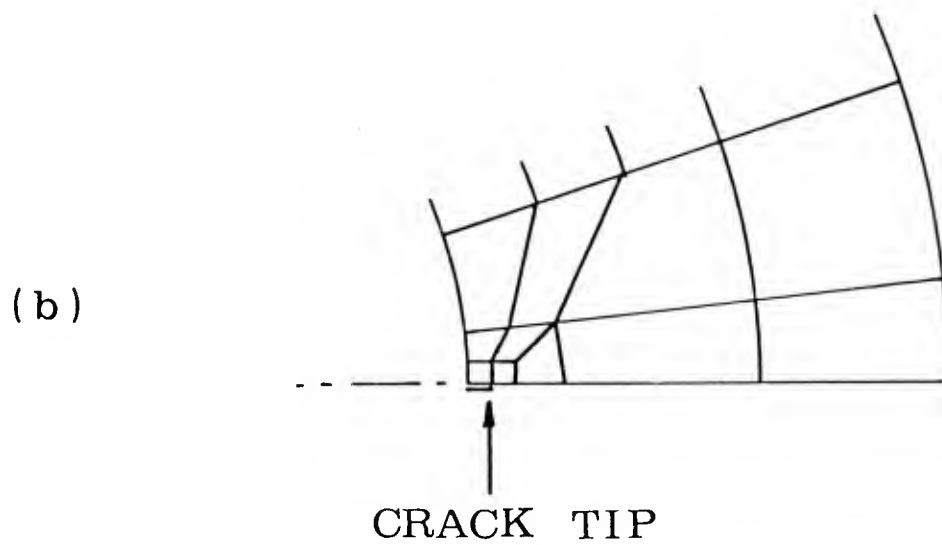


Figure 1(b). Idealization for very shallow cracks.

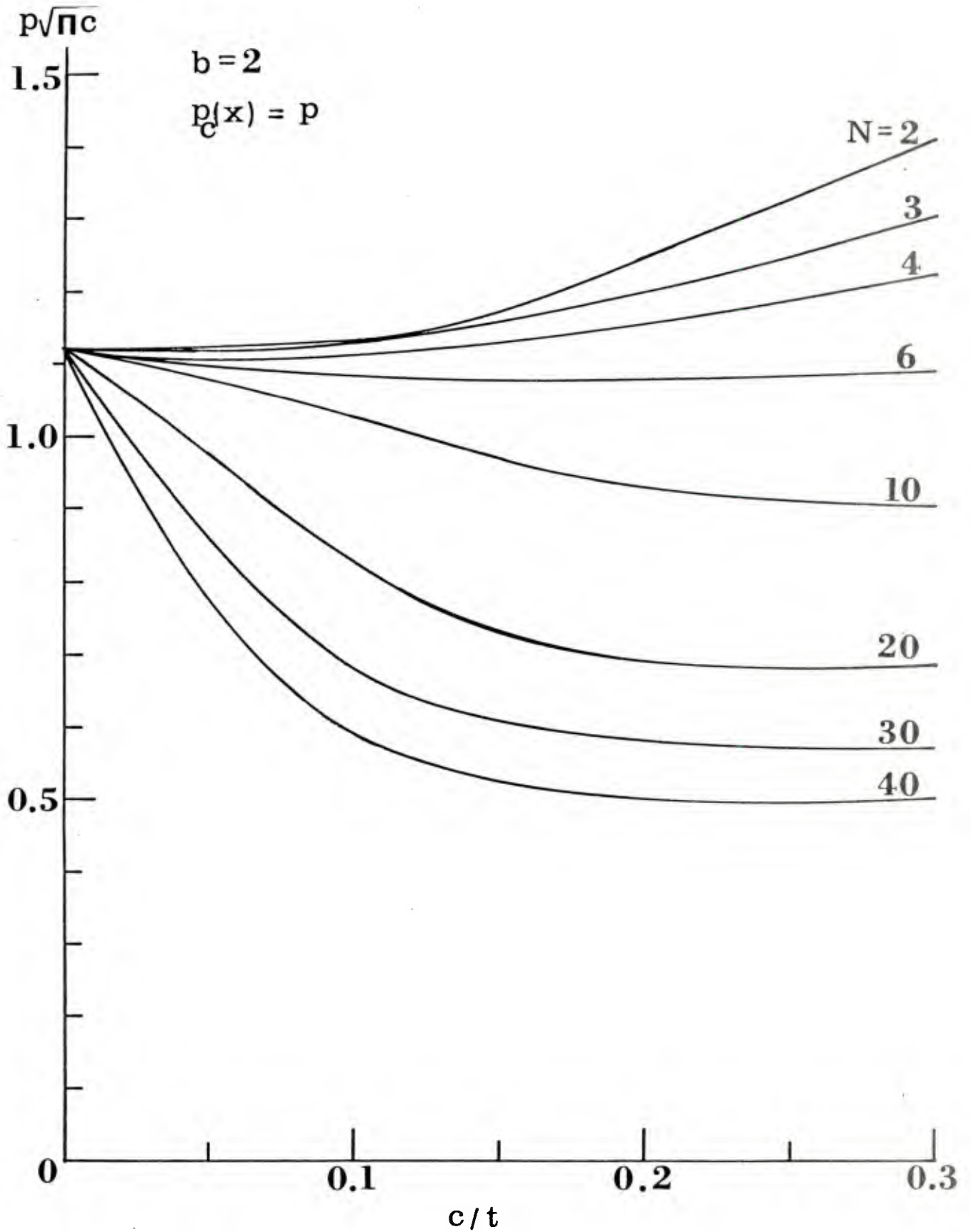


Figure 2. Stress intensity factors as a function of c/t for N radial cracks subjected to the crack face pressure $p_c(x) = p$.

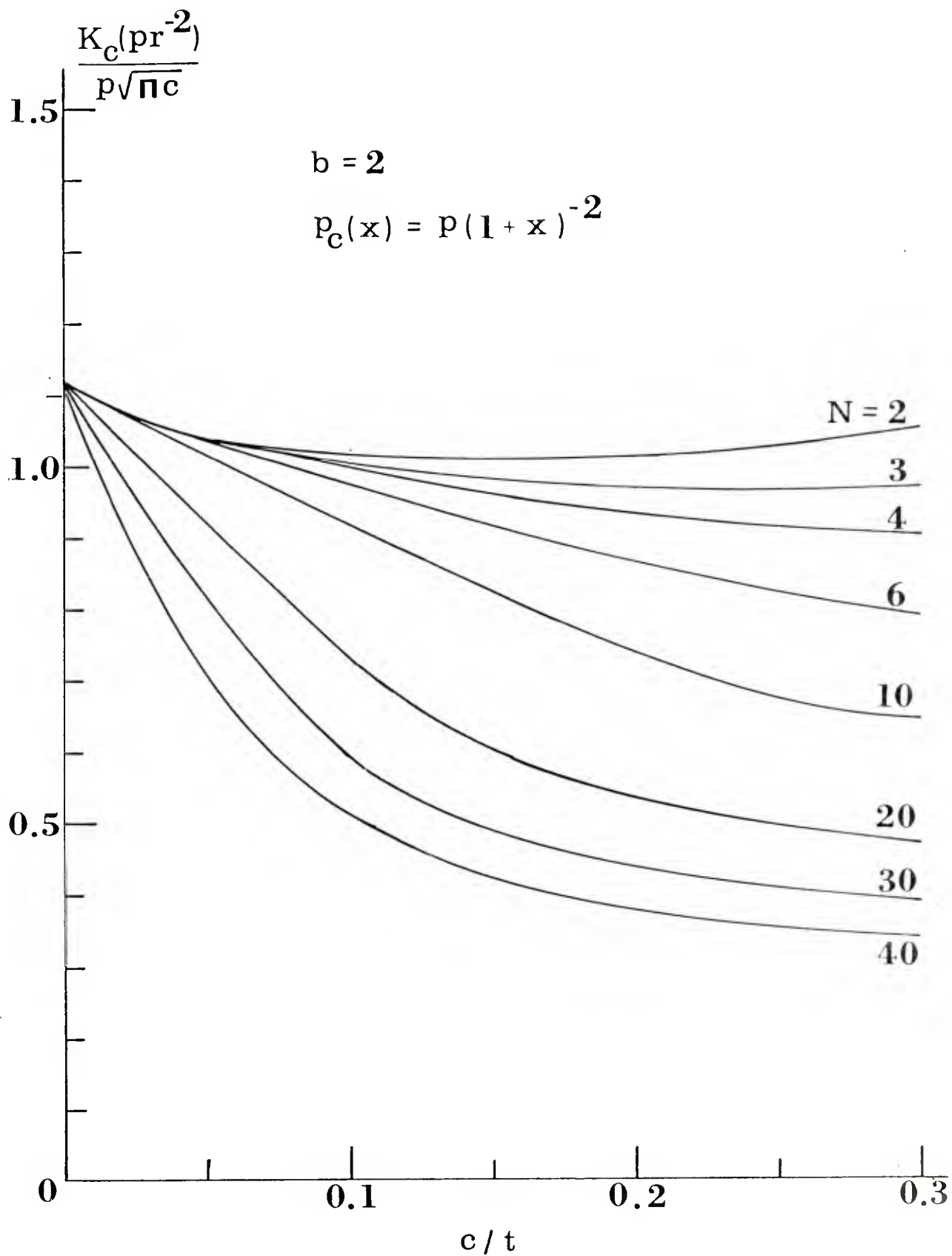


Figure 3. Stress intensity factors as a function of c/t for N radial cracks subjected to the crack face pressure $p_c(x) = p(1+x)^{-2}$.

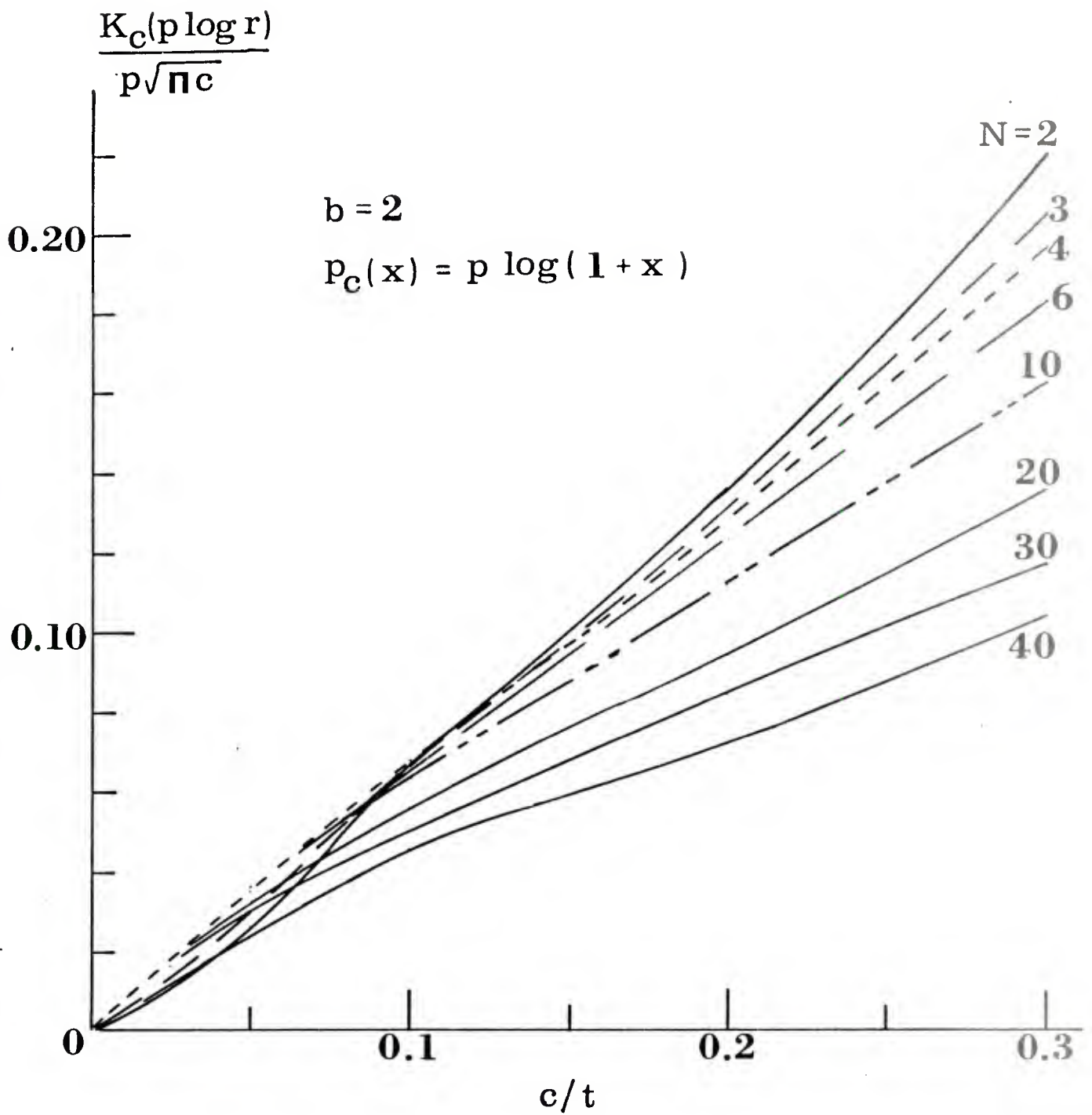


Figure 4. Stress intensity factors as a function of c/t for N radial cracks subjected to the crack face pressure $p_c(x) = p \log(1+x)$.

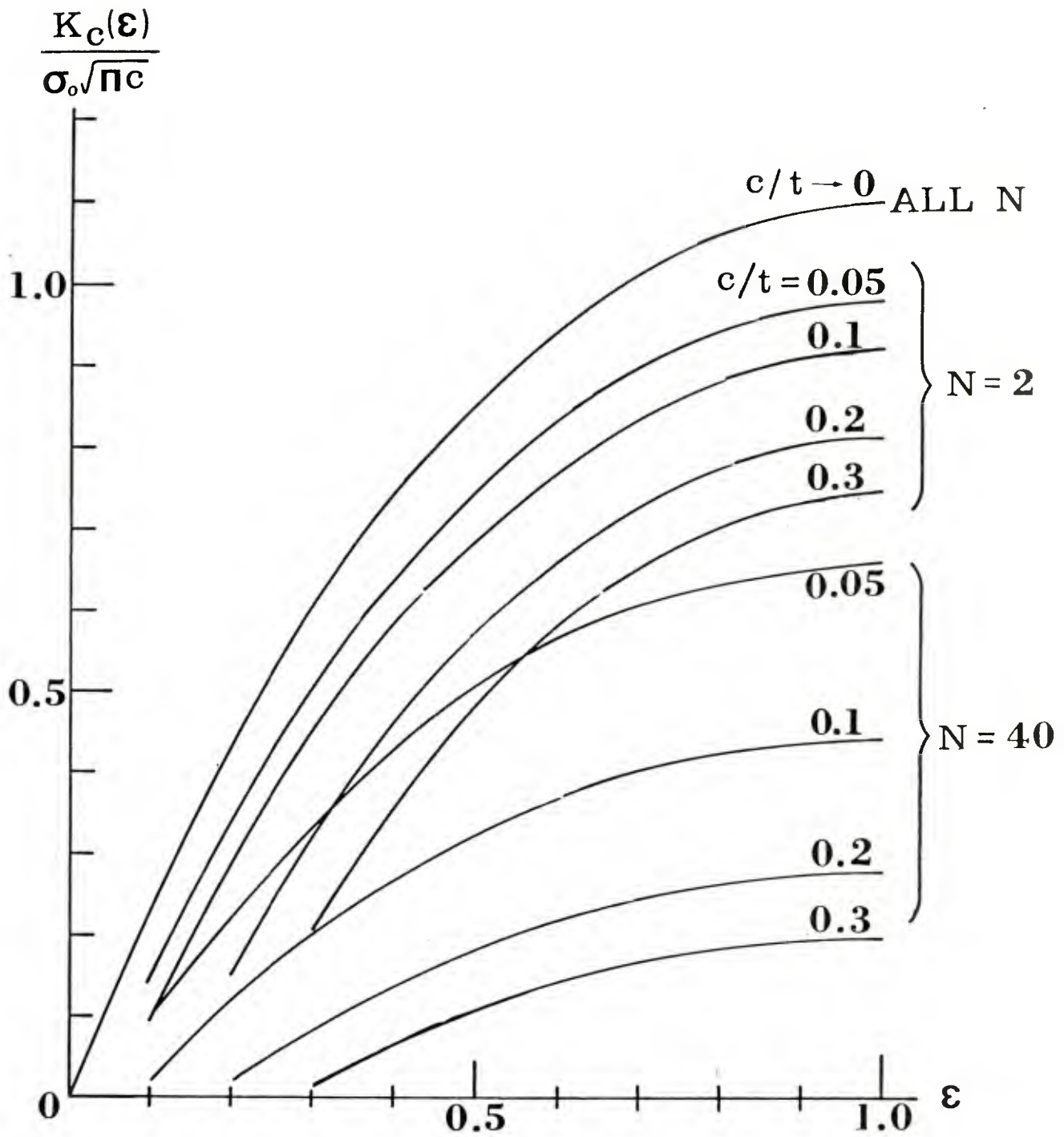


Figure 5. Stress intensity factors as a function of ϵ in an autofrettaged cylinder of $b = 2$.

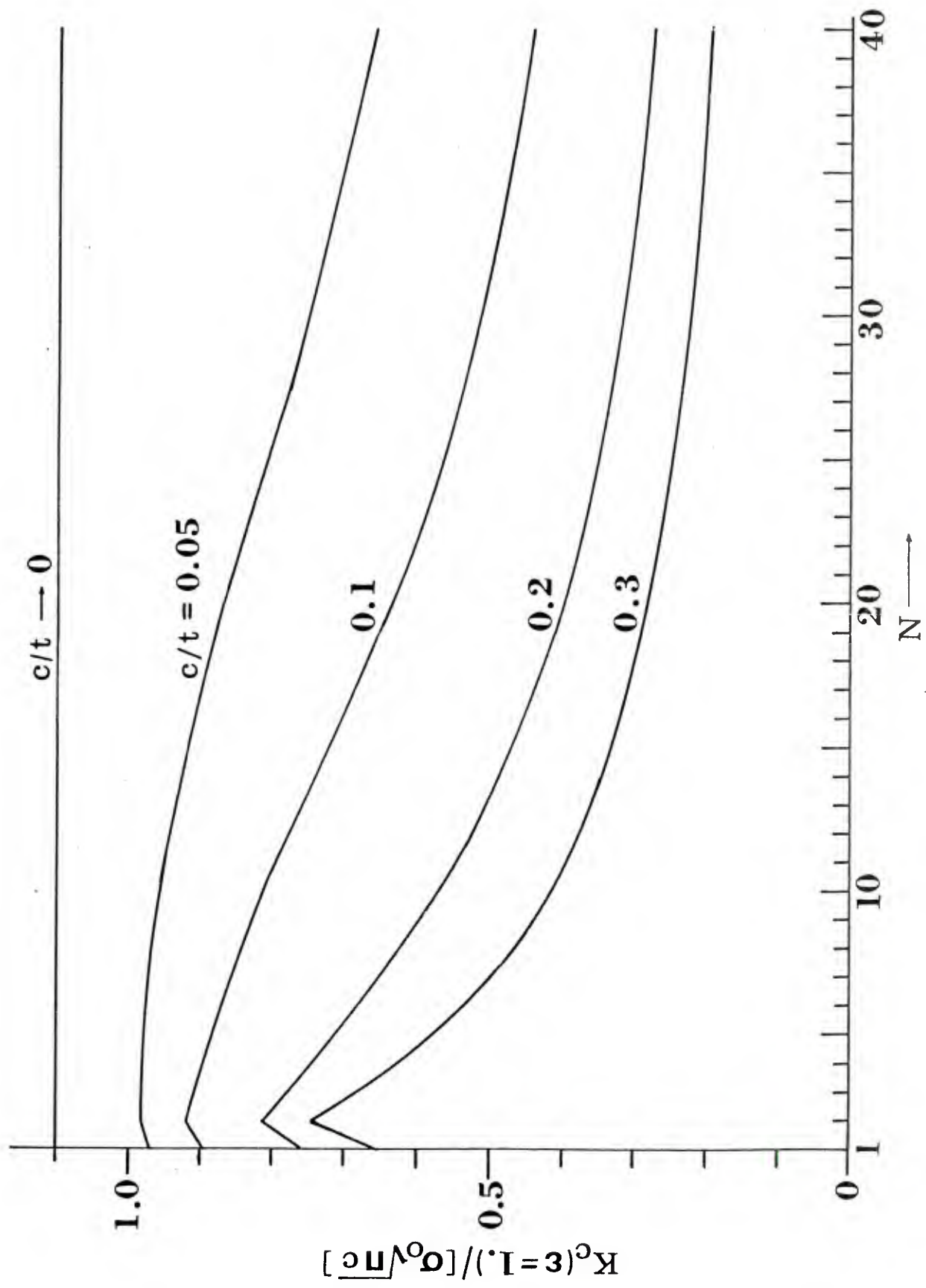


Figure 6. Stress intensity factors as a function of N in a fully autofretted cylinder of $b = 2$.

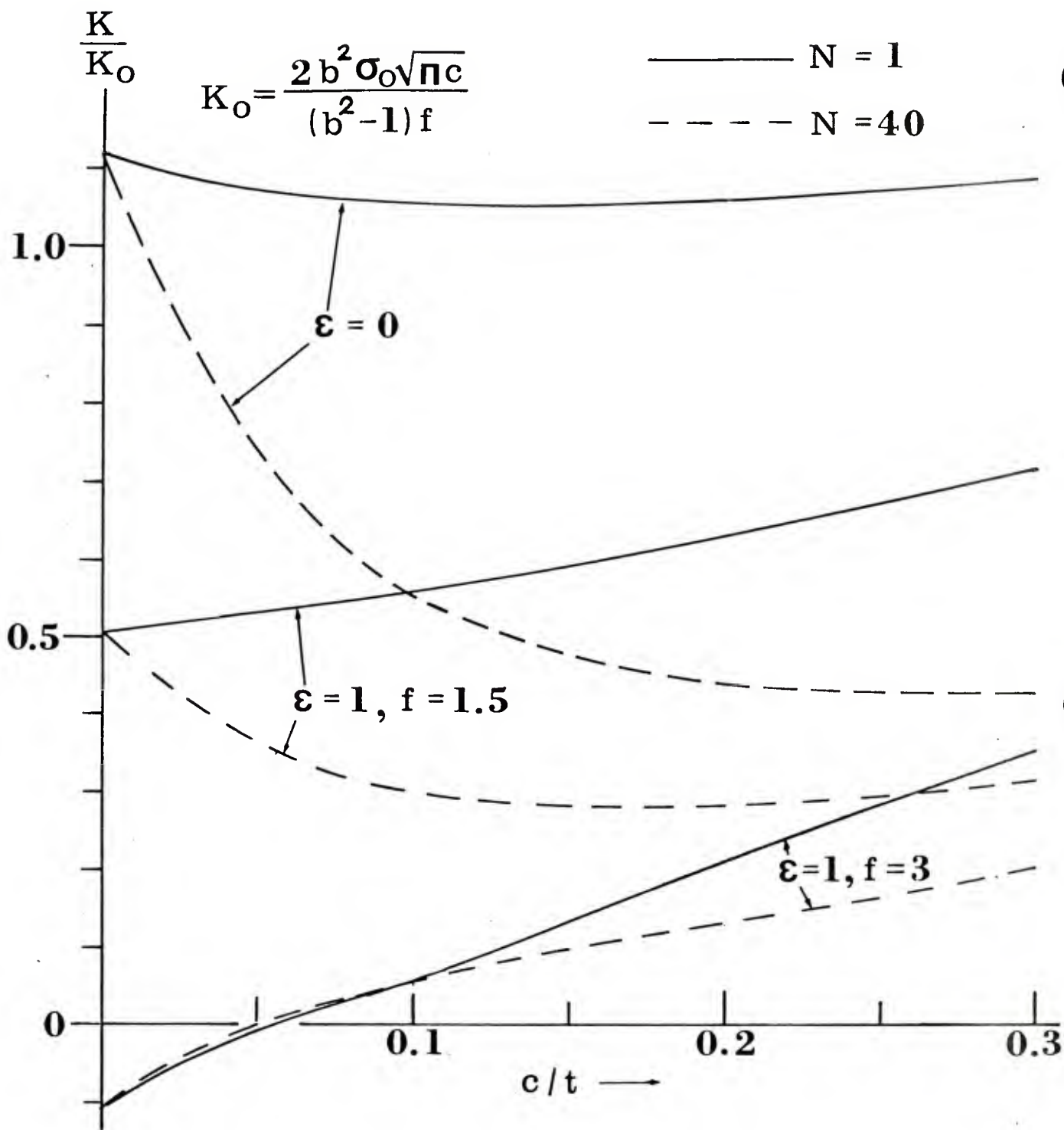


Figure 7. Stress intensity factors in an autofrettaged cylinder of $b = 2$ subjected to internal pressure σ_0/f on ID and on crack faces.

TECHNICAL REPORT INTERNAL DISTRIBUTION LIST

	<u>NO. OF COPIES</u>
COMMANDER	1
CHIEF, DEVELOPMENT ENGINEERING BRANCH	1
ATTN: DRDAR-LCB-DA	1
-DM	1
-DP	1
-DR	1
-DS	1
-DC	1
CHIEF, ENGINEERING SUPPORT BRANCH	1
ATTN: DRDAR-LCB-SE	1
-SA	1
CHIEF, RESEARCH BRANCH	2
ATTN: DRDAR-LCB-RA	1
-RC	1
-RM	1
-RP	1
CHIEF, LWC MORTAR SYS. OFC.	1
ATTN: DRDAR-LCB-M	
CHIEF, IMP. 81MM MORTAR OFC.	1
ATTN: DRDAR-LCB-I	
TECHNICAL LIBRARY	5
ATTN: DRDAR-LCB-TL	
TECHNICAL PUBLICATIONS & EDITING UNIT	2
ATTN: DRDAR-LCB-TL	
DIRECTOR, OPERATIONS DIRECTORATE	1
DIRECTOR, PROCUREMENT DIRECTORATE	1
DIRECTOR, PRODUCT ASSURANCE DIRECTORATE	1

NOTE: PLEASE NOTIFY ASSOC. DIRECTOR, BENET WEAPONS LABORATORY, ATTN:
DRDAR-LCB-TL, OF ANY REQUIRED CHANGES.

TECHNICAL REPORT EXTERNAL DISTRIBUTION LIST (CONT.)

	<u>NO. OF COPIES</u>		<u>NO. OF COPIES</u>
COMMANDER US ARMY RESEARCH OFFICE P.O. BOX 12211 RESEARCH TRIANGLE PARK, NC 27709	1	COMMANDER DEFENSE TECHNICAL INFO CENTER ATTN: DTIA-TCA CAMERON STATION ALEXANDRIA, VA 22314	12
COMMANDER US ARMY HARVEY DIAMOND LAB ATTN: TECH LIB 2800 POWDER MILL ROAD ADELPHIA, ME 20783	1	METALS & CERAMICS INFO CEN BATTELLE COLUMBUS LAB 505 KING AVE COLUMBUS, OHIO 43201	1
DIRECTOR US ARMY INDUSTRIAL BASE ENG ACT ATTN: DRXPE-MT ROCK ISLAND, IL 61201	1	MECHANICAL PROPERTIES DATA CTR BATTELLE COLUMBUS LAB 505 KING AVE COLUMBUS, OHIO 43201	1
CHIEF, MATERIALS BRANCH US ARMY R&S GROUP, EUR BOX 65, FPO N.Y. 09510	1	MATERIEL SYSTEMS ANALYSIS ACTV ATTN: DRXSY-MP ABERDEEN PROVING GROUND MARYLAND 21005	1
COMMANDER NAVAL SURFACE WEAPONS CEN ATTN: CHIEF, MAT SCIENCE DIV DAHLGREN, VA 22448	1		
DIRECTOR US NAVAL RESEARCH LAB ATTN: DIR, MECH DIV CODE 26-27 (DOC LIB) WASHINGTON, D. C. 20375	1 1		
NASA SCIENTIFIC & TECH INFO FAC. P. O. BOX 3757, ATTN: ACQ BR BALTIMORE/WASHINGTON INTL AIRPORT MARYLAND 21240	1		

NOTE: PLEASE NOTIFY COMMANDER, ARRADCOM, ATTN: BENET WEAPONS LABORATORY, DRDAF--LCB-TL, WATERVLIET ARSENAL, WATERVLIET, N.Y. 12189, OF ANY REQUIRED CHANGES.

TECHNICAL REPORT EXTERNAL DISTRIBUTION LIST

	<u>NO. OF COPIES</u>		<u>NO. OF COPIES</u>
ASST SEC OF THE ARMY RESEARCH & DEVELOPMENT ATTN: DEP FOR SCI & TECH THE PENTAGON WASHINGTON, D.C. 20315	1	COMMANDER US ARMY TANK-AUTMV R&D COMD ATTN: TECH LIB - DRDTA-UL MAT LAB - DRDTA-RK WARREN, MICHIGAN 48090	1 1
COMMANDER US ARMY MAT DEV & READ. COMD ATTN: DRDDE 5001 EISENHOWER AVE ALEXANDRIA, VA 22333	1	COMMANDER US MILITARY ACADEMY ATTN: CHMN, MECH ENGR DEPT WEST POINT, NY 10996	1
COMMANDER US ARMY ARRADCOM ATTN: DRDAR-LC -LCA (PLASTICS TECH EVAL CEN) -LCE -LCM -LCS -LCW -TSS (STINFO) DOVER, NJ 07801	1 1 1 1 1 2	US ARMY MISSILE COMD REDSTONE SCIENTIFIC INFO CEN ATTN: DOCUMENTS SECT, BLDG 4484 REDSTONE ARSENAL, AL 35898 COMMANDER REDSTONE ARSENAL ATTN: DRSMI-RRS -RSM ALABAMA 35809	2 1 1
COMMANDER US ARMY ARRCOM ATTN: DRSAR-LEP-L ROCK ISLAND ARSENAL ROCK ISLAND, IL 61299	1	COMMANDER ROCK ISLAND ARSENAL ATTN: SARRI-ENM (MAT SCI DIV) ROCK ISLAND, IL 61202	1
DIRECTOR US ARMY BALLISTIC RESEARCH LABORATORY ATTN: DRDAR-TSB-S (STINFO) ABERDEEN PROVING GROUND, MD 21005	1	COMMANDER HQ, US ARMY AVN SCH ATTN: OFC OF THE LIBRARIAN FT RUCKER, ALABAMA 36362	1
COMMANDER US ARMY ELECTRONICS COMD ATTN: TECH LIB FT MONMOUTH, NJ 07703	1	COMMANDER US ARMY FGN SCIENCE & TECH CEN ATTN: DRXST-SD 220 7TH STREET, N.E. CHARLOTTESVILLE, VA 22901	1
COMMANDER US ARMY MOBILITY EQUIP R&D COMD ATTN: TECH LIB FT BELVOIR, VA 22060	1	COMMANDER US ARMY MATERIALS & MECHANICS RESEARCH CENTER ATTN: TECH LIB - DRXMR-PL WATERTOWN, MASS 02172	2

NOTE: PLEASE NOTIFY COMMANDER, ARRADCOM, ATTN: BENET WEAPONS LABORATORY, DRDAR-LCB-TL, WATERVLIET ARSENAL, WATERVLIET, N.Y. 12189, OF ANY REQUIRED CHANGES.